Dalton Transactions

Accepted Manuscript

ROYAL SOCIETY OF CHEMISTRY

www.rsc.org/dalton

Dalton Transactions

Dynamic Article Links ▶

Cite this: DOI: 10.1039/c4dt00000x

www.rsc.org/Dalton Trans.

ARTICLE

Structural Diversities and Related Properties of Four Coordination Polymers Synthesized From Original Ligand of 3,3',5,5'-Azobenzenetetracarboxylic Acid

Liming Fan,[a,b] Weiliu Fan,[a] Bin Li,[b] Xinzheng Liu,[b] Xian Zhao*[a] and Xiutang Zhang*[a,b]

Received (in XXX, XXX) Xth XXXXXXXXX 2014, Accepted Xth XXXXXXXXX 2014
DOI: 10.1039/c4dt00000x

ABSTRACT: Four new coordination polymers, namely $[Co(H_2O_2abtc)(bibp)]_n$ (**1**), $\{[Mn_{1.5}(Oabtc)(H_2O)_2]\cdot(H_2bmib)_{0.5}\cdot H_2O\}_n$ (**2**), $\{[Cd_{1.5}(O_2abtc)]\cdot(H_2bmib)_{0.5}\cdot 2H_2O\}_n$ (**3**), and $\{[Cd(nip)(bibp)]\cdot 0.5H_2O\}_n$ (**4**), were constructed under solvothermal conditions in the presence of two bis(imidazole) bridging linkers (bimb = 1,4-bis(2-methylimidazol-1-ylmethyl)benzene, bibp = 4,4'-bis(imidazol-1-yl)biphenyl). The unstable azo ligand of 3,3',5,5'-azobenzenetetracarboxylic acid (H_4abtc) can be oxidized and reuslted in three oxidized derivatives of H_4Oabtc (one N atom was oxidized), H_4O_2abtc (two N atoms were oxidized), and H_2nip (One H_4abtc was oxidized into two 5-nitroisophthalic acid). Their structures have been determined by single-crystal X-ray diffraction analyses and further characterized by elemental analyses, IR spectra, powder X-ray diffraction (PXRD), and thermogravimetric (TG) analyses. Complex **1** exhibits an interestingly 2D+2D→3D parallel entangled networks based on 4-connected $(4^4.6^2)$-**sql** sheets. Complex **2** is a $\{Mn_3(COO)_6\}$ trinuclear SBUs based 2D (3,6)-connected $(4^3)_2(4^6\cdot 6^6\cdot 8^3)$-**kgd** sheet. While complex **3** displays a $\{Cd_3(COO)_8\}$ trinuclear SBUs based 3D (4,8)-connected $(4^6)_2(4^{12}\cdot 6^{12}\cdot 8^4)$-**flu** network. Complex **4** can be regard as a $\{Cd_2(COO)_2\}$ binuclear SBUs based 6-connected $(4^4\cdot 6^{11})$-**6T8** framework. Besides, the magenetic property of complexes **1**, **2** and the luminescence properties of complexes **3**, **4** have been investigated.

Introduction

The coordination polymers (CPs), as novel crystalline functional materials, often constructed from the organic ligands and inorganic nodes, have attracted upsurging research interest worldwidly.[1-3] Generally, the synthesis methods of such materials can be mainly divided into three categories: hydrothermal/solvothermal, evaporation, and diffusion.[4] Compared with other methods, the hydrothermal/solvothermal method seems more efficiently and used more widely, or even give us unexpected surprise, which can attribute to its advantages over other methods, such as, high temperature, high pressure, lower solvent viscosity, and thermodynamic control.[5]

We all known, the hydrothermal/solvothermal reactions are very complex processes, the starting materials dissolved in the solvent and interacted with each other under high temperature and pressure, finally given the thermodynamic products. When the hydrothermal/solvothermal method was used to obtain CPs, both the inorganic and organic building blocks will adjust themselves to satisfy the needs of the lowest energy principle.[6] The inorganic ions can be oxidized to the higher oxidation state, reduced to lower oxidation state, or even gathered together to form polymetallic clusters.[7,8] For the organic linkers, except the most commonly twisting, folding, and binding of backbones, they can be oxidized, reduced, decarboxylated, or rearrangement, finally given novel redecorating organic ligands.[9] Although many CPs have been constructed, and some organic ligands are rebuild during the hydrothermal/solvothermal reactions, the systematic studies of the relationship between the derivatives and final structures are rarely documented up to now.

Azo compounds, named after the azo group (–N=N–), have been widly used in dyeing industry. Azo compounds have *cis*– and *trans*– geometric isomers, which can be interchangeable in the light or heating conditions, and the *cis*–Azo are more stable. Besides, the azo group is easily oxidized by the oxygen in the air. Those features inspired us to select the 3,3',5,5'-azobenzenetetracarboxylic acid (H_4abtc) as building pillars to construct the CPs,[10] and investigated the chages of this ligand and the relationship between the H_4abtc oxidized derivatives and the final crystal structures. Moreover, the ancially bis(imidazole) linkers were selcted as the coligands, beacase the mixed ligands strategy make the assembly more easily.[11,12]

Herein, we reported three H_4abtc oxidized derivatives under solvothermal conditions and the depended coordination polymers, $[Co(H_2O_2abtc)(bibp)]_n$ (**1**),

[a] *State Key Laboratory of Crystal Materials, Shandong University , Jinan 250100, China. E-mail: zhaoxian@icm.sdu.edu.cn.*
[b] *Advanced Material Institute of Research, College of Chemistry and Chemical Engineering, Qilu Normal University, Jinan, 250013, China. E-mail: xiutangzhang@163.com.*

†Electronic Supplementary Information (ESI) available: Powder XRD patterns, TG curves, and X-ray crystallographic data, CCDC-1027723 for **1**, 1027724 for **2**, 1027725 for **3**, and 1027726 for **4**. See DOI: 10.1039/c4dt00000x.

$\{[Mn_{1.5}(Oabtc)(H_2O)_2]\cdot(H_2bmib)_{0.5}\cdot H_2O\}_n$ (**2**), $\{[Cd_{1.5}(O_2abtc)]\cdot(H_2bmib)_{0.5}\cdot 2H_2O\}_n$ (**3**), and $\{[Cd(nip)(bibp)]\cdot 0.5H_2O\}_n$ (**4**), which exhibit a systematic variation of architectures from 2D (3,6)-connected **kgd** sheet (**2**), 2D+2D→3D 4-connected **sql** parallel entangled network (**1**), 3D (4,8)-connected **flu** net (**3**), to 3D 6-connected **6T8** framework (**4**). These results revealed that H_4abtc ligands can be oxidized under solvothermal conditions (Scheme 1) and its oxidized derivatives have great influence on the final structures.

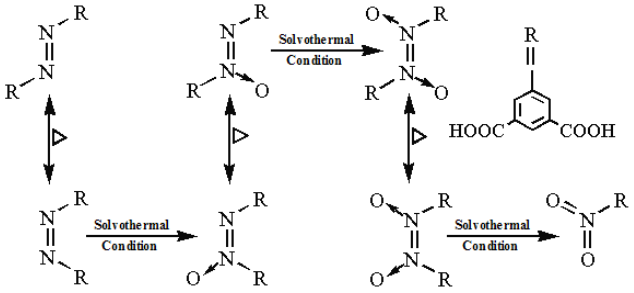

Scheme 1. The possible oxidation process of H_4abtc ligand under solvothermal conditions.

Experimental Section

Materials and Methods. All the chemical reagents were purchased from Jinan Henghua Sci. & Tec. Co. Ltd. without further purification. IR spectra were measured on a NEXUS 670 FTIR spectrometer at the range of 600-4000 cm^{-1}. Elemental analyses were carried out on a CE instruments EA 1110 elemental analyzer. TGA was measured from 25 to 800 ^oC on a SDT Q600 instrument at a heating rate 5 ^oC/min under the N_2 atmosphere (100 mL/min). X-ray powder diffractions were measured on a Panalytical X-Pert pro diffractometer with Cu-Kα radiation. The variable-temperature magnetic susceptibility measurements were performed on the Quantum Design SQUID MPMS XL-7 instruments in the temperature range of 2-300 K under a field of 1000 Oe. Fluorescence spectra were performed on a Hitachi F-4500 fluorescence spectrophotometer at room temperature.

General Synthesis and Characterization. All the titled compelxes are synthesised under simialr conditions with the mixture of H_4abtc, ancillary imidazole linkers (bmib or bibp), and transitional metal salts added in the mixed sovlents. The NaOH was added to eliminate the protons of H_4abtc. To check the phase purity of **1**−**4**, PXRD has been introduced, the comparisons of measured and simulated PXRD patterns shows the main peaks are aligned with each other, which indicated the high purity of those complexes (Fig. S1). For **1**−**4**, the IR absorption bands in the range of 3400-3500 cm^{-1} can be attributed to the characteristic peaks of O-H vibrations. The vibrations at ca. 1530 and 1620 cm^{-1} correspond to the asymmetric and symmetric stretching vibrations of the carboxyl groups, respectively.

Synthesis of $[Co(H_2O_2abtc)(bibp)]_n$ (1). The mixture of H_4abtc (0.15 mmol, 0.054 g), bibp (0.20 mmol, 0.052 g), $Co(NO_3)_2\cdot 6H_2O$ (0.40 mmol, 0.116 g), NaOH (0.30 mmol, 0.012 g), 12 mL H_2O and 2 mL ethanol were stirred continually for 1 h and then transfered to the 25 mL Teflon-lined stainless steel vessel, heated to 170 °C for 3 days, followed by slow cooling (a descent rate of 10 ^oC/h) to room temperature. Purple block crystals of **1** were obtained. Yield of 57% (based on H_4abtc). Anal. (%) calcd. for $C_{34}H_{22}CoN_6O_9$: C, 56.91; H, 3.09; N, 11.71. Found: C, 56.37; H, 3.37; N, 11.89. IR (KBr pellet, cm^{-1}): 3421 (s), 3103 (m), 1631 (vs), 1564 (vs), 1474 (s), 1440 (s), 1357 (vs), 1247 (m), 768 (m), 731 (s), 523 (w).

Synthesis of $\{[Mn_{1.5}(Oabtc)(H_2O)_2]\cdot(H_2bmib)_{0.5}\cdot H_2O\}_n$ (2). The mixture of H_4abtc (0.15 mmol, 0.054 g), bmib (0.20 mmol, 0.053 g), $MnSO_4\cdot H_2O$ (0.40 mmol, 0.068 g), NaOH (0.30 mmol, 0.012 g), 12 mL H_2O and 2 mL ethanol were stirred continually for 1 h and then transfered to the 25 mL Teflon-lined stainless steel vessel, heated to 170 °C for 3 days, followed by slow cooling (a descent rate of 10 ^oC/h) to room temperature. Light orange block crystals of **2** were obtained. Yield of 72% (based on H_4abtc). Anal. (%) calcd. for $C_{48}H_{42}Mn_3N_8O_{24}$: C, 45.05; H, 3.31; N, 8.76. Found: C, 44.78; H, 3.47; N, 8.67. IR (KBr pellet, cm^{-1}): 3429 (s), 1647 (vs), 1623 (s), 1579 (m), 1431 (s), 1371 (s), 897 (m), 773 (s), 527 (w).

Synthesis of $\{[Cd_{1.5}(O_2abtc)]\cdot(H_2bmib)_{0.5}\cdot 2H_2O\}_n$ (3). The same synthetic procedure as for complex **2** was used except the $MnSO_4\cdot H_2O$ (0.40 mmol, 0.068 g) was replaced by the $3CdSO_4\cdot 8H_2O$ (0.13 mmol, 0.102 g). Finally giving colorless block crystals of **3** with the yield of 62% (based on H_4abtc). Anal. (%) calcd. for $C_{48}H_{36}Cd_3N_8O_{20}$: C, 41.71; H, 2.63; N, 8.11. Found: C, 41.07; H, 3.03; N, 7.98. IR (KBr pellet, cm^{-1}): 3439 (s), 3228 (s), 1649 (s), 1621 (vs), 1572 (m), 1530 (w), 1381 (s), 1347 (w), 1202 (m), 1107 (w), 842 (m), 741(m), 529 (w).

Synthesis of $\{[Cd(nip)(bibp)]\cdot 0.5H_2O\}_n$ (4). The same synthetic procedure as for complex **1** was used except the $Co(NO_3)_2\cdot 6H_2O$ (0.40 mmol, 0.116 g) was replaced by the $3CdSO_4\cdot 8H_2O$ (0.13 mmol, 0.102 g). Finally giving colorless block crystals of **4** with the yield of 49% (based on H_4abtc). Anal. (%) calcd. for $C_{26}H_{18}CdN_5O_{6.5}$: C, 50.62; H, 2.94; N, 11.35. Found: C, 49.87; H, 3.11; N, 10.97. IR (KBr pellet, cm^{-1}): 3428 (m), 1618 (s), 1513 (s), 1450 (m), 1339 (s), 1257 (m), 1063 (s), 862 (m), 821 (m), 727 (m), 645 (s), 517 (m).

X-ray crystallography. Intensity data collection was carried out on a Siemens SMART diffractometer equipped with a CCD detector using Mo-*Kα* monochromatized radiation (λ = 0.71073 Å) at 273(2) K. The absorption correction was based on multiple and symmetry-equivalent reflections in the data set using the SADABS program based on the method of Blessing. The structures were solved by direct methods and refined by full-matrix least-squares using the SHELXTL package.[14] The O atoms in azo group of complex **1** are disordered and were refined with an occupancy ratio of 80:20 for O5 and O5'. And the occupancy ratio of O8 (O4) of complex **2** are 30:70. For complex **3**, the O9 and O10 in azo groupare disordered and were refined with an occupancy ratio of 48:52. And the occupancy ratio of O1w of complex **4** are 50. Crystallographic data for complexes **1**–**4** are given in Table 1. Selected bond lengths and angles for **1**–**4** are listed in Table S1. For complexes of **1**–**4**, further details of the crystal structure can be obtained from the Cambridge Crystallographic Data Centre, CCDC, 12 Union Road, CAMBRIDGE CB2 1EZ, UK, [Telephone:+44-(0)1223-762-910, Fax: +44-(0)1223-336-033; E-mail: deposit@ccdc.cam.ac.uk, http://www.ccdc.cam.ac.uk/deposit], on quoting the depository number CCDC-1027723 for **1**, 1027724 for **2**, 1027725 for **3**, and 1027726 for **4**.

Table 1 Crystal data for **1–4**

Compound	**1**	**2**	**3**	**4**
Empirical formula	$C_{34}H_{22}CoN_6O_9$	$C_{48}H_{42}Mn_3N_8O_{24}$	$C_{48}H_{36}Cd_3N_8O_{20}$	$C_{26}H_{18}CdN_5O_{6.5}$
Formula weight	717.51	1279.72	1382.05	616.85
Crystal system	Monoclinic	Triclinic	Triclinic	Monoclinic
Space group	$P2_1/c$	P-1	P-1	$C2/c$
a (Å)	11.8287(14)	9.7766(17)	9.973(2)	14.256(3)
b (Å)	16.996(2)	12.204(2)	10.452(2)	15.256(3)
c (Å)	15.0618(19)	12.262(2)	12.671(3)	23.920(4)
α (°)	90	72.090(3)	111.595(3)	90
β (°)	100.133(2)	85.517(3)	104.229(3)	101.486(3)
γ (°)	90	73.131(3)	92.999(3)	90
V(Å^3)	2980.8(6)	1332.1(4)	1175.4(4)	5098.3(15)
Z	4	1	1	8
D_{calcd} (Mg/m^3)	1.599	1.595	1.953	1.607
μ(mm^{-1})	0.647	0.794	1.440	0.910
T(K)	273(2)	273(2)	273(2)	273(2)
R_{int}	0.0515	0.0258	0.0179	0.0549
Final R indices[$I > 2\sigma(I)$]	$R_1 = 0.0563$, $wR_2 = 0.1553$	$R_1 = 0.0565$, $wR_2 = 0.1444$	$R_1 = 0.0329$, $wR_2 = 0.0861$	$R_1 = 0.0526$, $wR_2 = 0.1356$
R indices (all data)	$R_1 = 0.0871$, $wR_2 = 0.1753$	$R_1 = 0.0832$, $wR_2 = 0.1644$	$R_1 = 0.0419$, $wR_2 = 0.0909$	$R_1 = 0.0877$, $wR_2 = 0.1549$
Gof	1.002	1.069	1.052	1.036

$R_1 = \Sigma||F_o|-|F_c||/\Sigma|F_o|$, $wR_2 = [\Sigma w(F_o^2-F_c^2)^2]/\Sigma w(F_o^2)^2]^{1/2}$

Result and Discussion

Structural Description of $[Co(H_2O_2abtc)(bibp)]_n$ (1). Structural analysis reveals that one N_{azo} atom in H_4abtc was oxidized, and H_4O_2abtc is partially deprotonated and acts as the bridging linker, finally resulting in an interestingly 2D+2D→3D parallel entangled network with the help of bibp. Complex **1** crystallizes in the monoclinic system, space group $P2_1/c$. As shown in the Fig. 1a, the asymmetric unit consists of one Co^{II} ion, one $H_2O_2abtc^{2-}$, and one bibp molecule. The coordination sphere of each Co^{II} centre is defined by two carboxyl O atoms and two N atoms, showing a distorted [CoN_2O_2] tetrahedral coordination environment. The Co−N bond distances [Co(1)–N(3) = 2.035(4) Å, and Co(1)–N(6)B = 2.004(3) Å] are longer than that of Co−O [Co(1)–O(1) = 1.993(3) Å, and Co(1)–O(8)A = 1.942(3) Å], indicating the band lengths of Co–O are stronger than those of Co–N.

The partially deprotonated $H_2O_2abtc^{2-}$ acts as pillars and connects Co^{II} ions *via* monodentate carboxyl groups (Mode I, Scheme 2), successfully offering a snake-like $[Co(H_2O_2abtc)]_n$ chain with the Co···Co distance and the Co···Co···Co angle being 14.097(7) Å and 74.14(0)°, respectively (Fig. 1b). Besides, the dihedral angle between two phenyl rings is 5.74(0)°, indicating the whole $H_2O_2abtc^{2-}$ ligand only has very slightly distortion. Along another direction, the bibp ligand adopts the *Cis-Cis* conformation to connect metal centres, leaving a 1D $[Co(bibp)]_n^{2n+}$ chain. And the bibp separated Co···Co distance is 17.438(1) Å, Co···Co···Co angle being 180.0° (Fig. 1b). The above two kinds of chains were hinged into 2D wave sheet by sharing the Co^{II} centres. The large void dimension of each sheet makes the interpenetration of adjacent sheets possible. The single 2D sheet interpenetrated with two neighbouring ones, finally forming a 2D+2D→3D parallel polycatenation network (Fig. 1c).

From the viewpoint of topology,[15] the $H_2O_2abtc^{2-}$ as well as bibp ligands act as bridging linkers, and the Co^{II} ions can be regarded as four-connected nodes. Thus, the overall network can be defined as a 4–connected $(4^4\cdot6^2)$–**sql** subunits based 2D+2D→3D parallel polycatenation network (Fig. 1d), which have been rarely reported because the 2D→3D parallel polycatenation need the single layer possessing a high undulation. Recent, Hong and co-workers have been reported $[Zn(H_2OL)(4,4'\text{-bpy})]_n$, exhibiting the similar structure.[10a] The difference between them is the building pillars in complex **1** is longer. The length expansion of the linkers gives an idea to systematic study the 2D→3D parallel polycatenation network.

Structural Description of $\{[Mn_{1.5}(Oabtc)(H_2O)_2]\cdot(H_2bmib)_{0.5}\cdot H_2O\}_n$ (2). Although the oxidized H_4abtc derivative in complex **2** is same with that in complex **1**, the final packing diagram exhibits an entirely different trinuclear $\{Mn_3(COO)_6\}$ SBUs based 2D **kgd** sheet due to the influence of guest bmib ligand. Complex **2** crystallizes in the triclinic system, space group P-1, and the asymmetric unit consisting of one and a half crystallographically independent Mn^{II} ions, one completely deprotonated $Oabtc^{4-}$, two coordinated water molecules, half a H_2bmib^{2+} ligands, and one lattice water molecule (Fig. 2a). Mn1 is hexacoordinated in a distorted octahedral coordination environment, defined by six O atoms from three different $Oabtc^{4-}$ ligands and two water molecules. Mn2 is centrosymmetric, located in octahedral coordination geometry, completed by six O atoms from six distinct $Oabtc^{4-}$ ligands. The Mn−O bond lengths are in the range of 2.125(8)–2.564(3) Å, similar with the above reported ones.[16a-c]

The completely deprotonated $Oabtc^{4-}$ ligand exhibits $(\kappa^1\text{-}\kappa^1)$-$(\kappa^0\text{-}\kappa^2)$-$(\kappa^1\text{-}\kappa^1)$-$\mu_6$ coordination mode (Mode II), with the dihedral angle between two phenyl rings being 76.76(2)°. The $(\kappa^1\text{-}\kappa^1)$-$\mu_2$ and $(\kappa^0\text{-}\kappa^2)$-$\mu_2$ carboxyl groups linked three Mn^{II} ions, successfully generating a trinuclear $\{Mn_3(COO)_6\}$ SBUs with Mn1···Mn2 distance being 3.441(7) Å (Fig. 2b). Each $\{Mn_3(COO)_6\}$ SBUs linked by six $Oabtc^{4-}$ ligand, finally obtaining a 2D layer (Fig. 2c). At the sight of topology, the packing layer can be defined as a (3,6)–connected **kgd** sheet with the Schläfli symbol of $(4^3)_2(4^6\cdot6^6\cdot8^3)$ by denoting the trinuclear $\{Mn_3(COO)_6\}$ SBUs to 6–connected nodes, and the $Oabtc^{4-}$ ligands to 3–connected nodes, respectively (Fig. 2d).

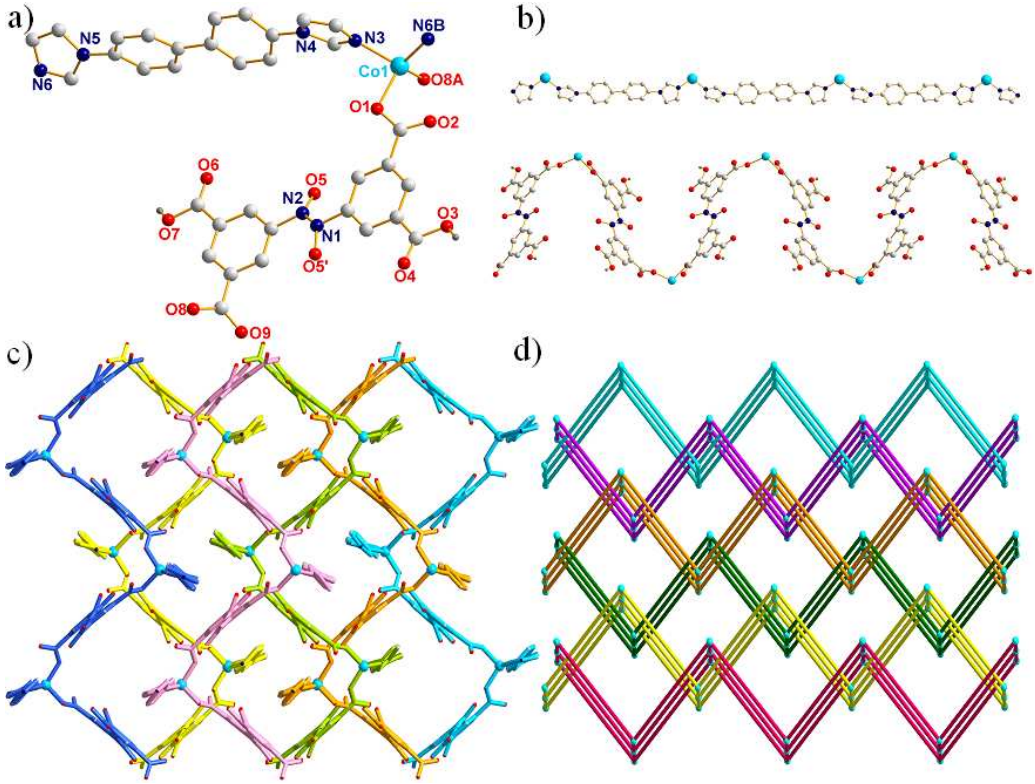

Figure 1. (a) Crystal structure of complex **1** (Symmetry codes: A: 1–*x*, –1/2+*y*, 1/2–*z*; B: 1+*x*, 1+*y*, *z*). (b) The 1D straight $[Co(bibp)]_n^{2n+}$ chain (the above) and $[Co(H_2O_2abtc)]_n$ snake chain (the below). (c) Schematic view of the 2D+2D→3D parallel polycatenation network in **1**. (d) The 4-connected **sql** subunits based 2D+2D→3D topology of **1** (green spheres: Co^{II} ions).

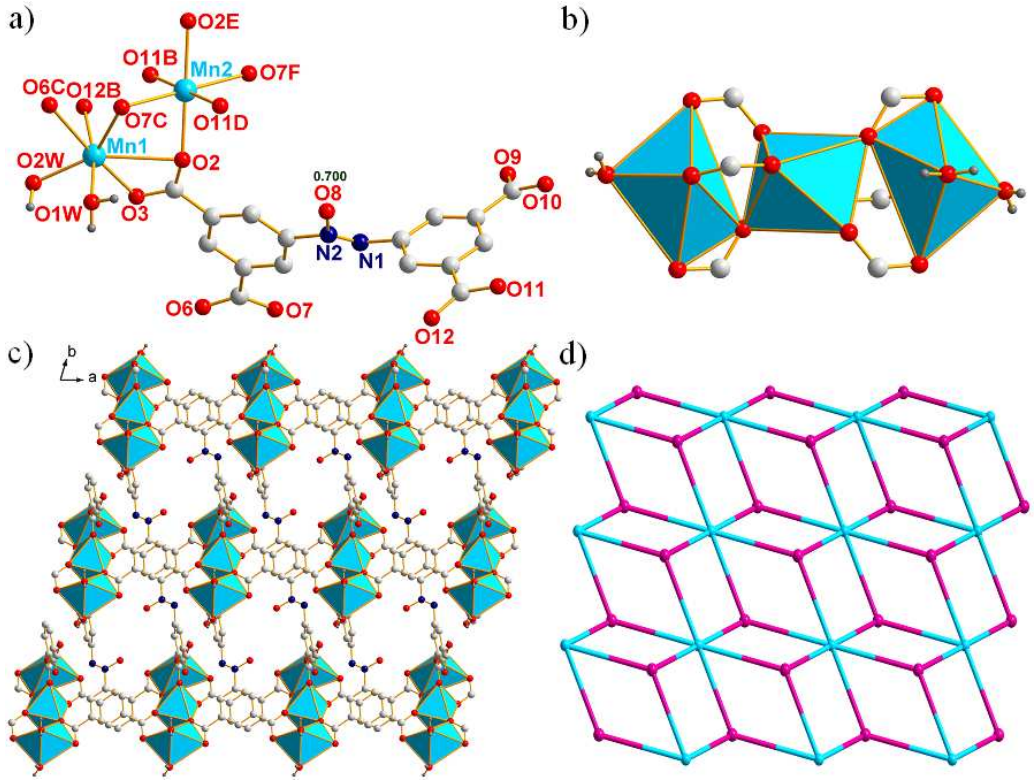

Figure 2 (a) Crystal structure of **2**, with the free ligand and lattice water molecules omitted (Symmetry codes: B: –1+*x*, 1+*y*, *z*; C: –1+*x*, *y*, *z*; D: 1–*x*, 1–*y*, 2–*z*; E:–*x*, 2–*y*, 2–*z*; F: 1–*x*, 2–*y*, 2–*z*.). (b) The $\{Mn_3(COO)_6\}$ trinuclear SBUs. (c) Schematic view of the 2D network of **2** along *c* axis. (d) The 2D (3,6)-connected $(4^3)_2(4^6{\cdot}6^6{\cdot}8^3)$-**kgd** sheet of **2** (green spheres: $\{Mn_3(COO)_6\}$ trinuclear SBUs; red spheres: Oabtc $^{4-}$ ligands).

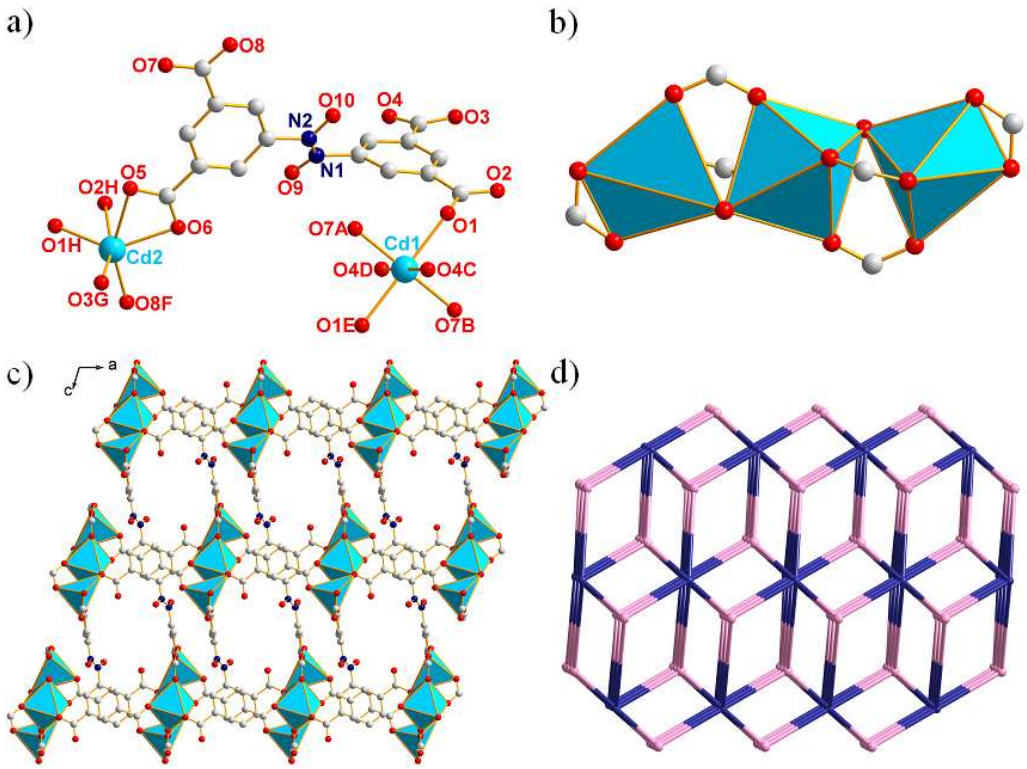

Figure 3 (a) Crystal structure of **3**, with the free ligand and lattice water molecules omitted (Symmetry codes: A: 1–*x*, 1–*y*, –*z*; B: *x*, *y*, 1+*z*; C: –1+*x*, *y*, *z*; D: 2–*x*, 1–*y*, 1–*z*; E: 1–*x*, 1–*y*, 1–*z*; F: *x*, –1+*y*, *z*; G: –1+*x*, –1+*y*, –1+*z*; H: *x*, –1+*y*, –1+*z*). (b) The $\{Cd_3(COO)_8\}$ trinuclear SBUs. (c) Schematic view of the 3D framework of **2**. (d) The 3D (4,8)-connected $(4^6)_2(4^{12}\cdot6^{12}\cdot8^4)$-**flu** net of **3** (green spheres: $\{Cd_3(COO)_8\}$ trinuclear SBUs; red spheres: O_2abtc^{4-} ligands).

Structural Description of $\{[Cd_{1.5}(O_2abtc)]\cdot(Hbmib)_{0.5}\cdot2H_2O\}_n$ (3). When two N_{azo} atoms of H_4abtc were oxidized, the final structure turned from trinuclear SBUs based 2D (3,6)-connected **kgd** sheet (**2**) to trinuclear SBUs based 3D (4,8)-connected **flu** net (**3**). Structural analysis reveals that complex **3** crystallizes in the triclinic system *P*-1. Complex **3** consists of one and a half crystallographically independent Cd^{II} ions, one O_2abtc^{4-} ligand, half of H_2bmib^{2+} ligands, and two lattice water molecules. As depicted in Fig. 3a, Cd1 is centrosymmetry, hexa-coordinated by six O atoms from six different O_2abtc^{4-} ligands, forming octahedral coordination geometry with slightly distorted. Cd2 is located in a distorted $[CdO_5]$ quadrangular pyramid environment, completed by five carboxyl O atoms from four O_2abtc^{4-} ligands. And the Cd−O bond lengths are in the range of 2.197(7)−2.394(5) Å, similar with the reported ones. [16d,e]

The O_2abtc^{4-} ligand can adjust themselves by rotating through the C−N bonds, and the dihedral angle between two phenyl rings is 81.48(2)°. The four carboxyl groups exhibiting $(\kappa^1\text{-}\kappa^1)\text{-}\mu_1$, $(\kappa^1\text{-}\kappa^1)\text{-}\mu_2$, $(\kappa^1\text{-}\kappa^2)\text{-}\mu_2$, and $(\kappa^1\text{-}\kappa^1)\text{-}\mu_2$ coordination modes (Mode III), linked with seven Cd^{II} ions. It is noteworthy that the $(\kappa^1\text{-}\kappa^1)\text{-}\mu_2$ as well as the $(\kappa^1\text{-}\kappa^2)\text{-}\mu_2$ carboxyl groups shared the Cd^{II} ions, obtained a trinuclear $\{Cd_3(COO)_8\}$ SBUs, with Cd1···Cd2 distance is 3.512 (8) Å (Fig. 3b). Compared with the trinuclear $\{Mn_3(COO)_6\}$ SBUs in complex **2**, we found the $\{Cd_3(COO)_8\}$ SBUs linked more carboxyl groups with the coordinated water molecules elimination. The trinuclear $\{Cd_3(COO)_8\}$ SBUs connected with eight different O_2abtc^{4-} ligands, constructed a 3D framework (Fig. 3c).

From the viewpoint of structural topology, the whole structure of complex **3** can be defined as a (4,8)–connected **flu** net with the Schläfli symbol of $(4^6)_2(4^{12}\cdot6^{12}\cdot8^4)$ by denoting the $Cd_3(COO)_8\}$ trinuclear SBUs to 8–connected nodes and O_2abtc^{4-} ligands to 4–connected nodes, respectively (Fig. 3d).

Structural Description of $\{[Cd(nip)(bibp)]\cdot0.5H_2O\}_n$ (4). One H_4abtc ligand was broken to two nip ligands when the two N atoms of azo group were oxidized. Structural analyses reveal that complex **4** is a $\{Cd_2(COO)_4\}$ binuclear SBUs based 3D framework, crystallizes in the monoclinic system, space group *C*2/c. As shown in Fig. 4a, there are one crystallographically independent Cd^{II} ion, one nip^{2-} ligand, one bibp ligand, and a half of lattice water molecules in the asymmetric unit. Each Cd^{II} centre is hexa-coordinated by two N atoms from different bibp ligands, and four O atoms from three nip^{2-} ligands, showing distorted octahedral coordination environment. Besides, the Cd−N bond lengths are 2.196(5) and 2.292(6) Å, the Cd−O bond lengths are in the range of 2.200(6)−2.629(5) Å, respectively.

The nip^{2-} ligand linked with three Cd^{II} ions by using the $(\kappa^1\text{-}\kappa^0)\text{-}(\kappa^1\text{-}\kappa^2)\text{-}\mu_3$ coordination mode (Mode IV). And two $(\kappa^1\text{-}\kappa^2)\text{-}\mu_2$ carboxyl groups linked two Cd^{II} ions, forming a binuclear $\{Cd_2(COO)_4\}$ binuclear SBUs, with the Cd···Cd distance is 3.780 (3) Å. The nip^{2-} ligands linked with the $\{Cd_2(COO)_4\}$ binuclear SBUs, leaving a 1D $[Cd(nip)]_n$ ladder chain (Fig. 4b), with the $N_{nitro}\cdots N_{nitro}$ distance of neighbouring chains is 3.280(4) Å. It is noteworthy that the bibp ligands connected with the Cd^{II} ions, forming a DNA-like $[Cd(bibp)]_n^{2n+}$ double helix chain, with the Cd···Cd distance being 17.435 (9) Å (Fig. 4b).

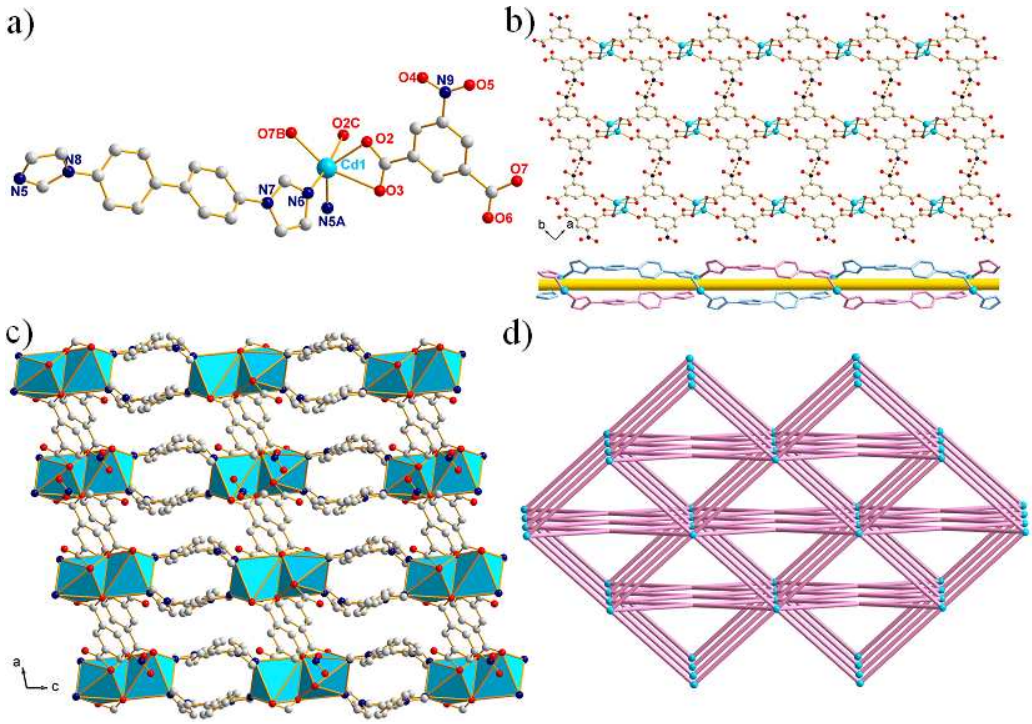

Figure 4 (a) Crystal structure of complex **4** (Symmetry codes: A: 1–*x*, –1+*y*, 1/2–*z*; B: 1/2+*x*, 1/2+*y*, *z*; C: 1–*x*, –*y*, 1–*z*). (b) The 1D ladder $[Cd(nip)]_n$ chain (the above) and right- and left- handed double helix $[Cd(bibp)]_n^{2n+}$ chains (the below). (c) Schematic view of the 3D framework in **4**. (d) The 3D 6-connected $(4^4{\cdot}6^{11})$-**6T8** net of **4** (green spheres: $\{Cd_2(COO)_4\}$ binuclear SBUs).

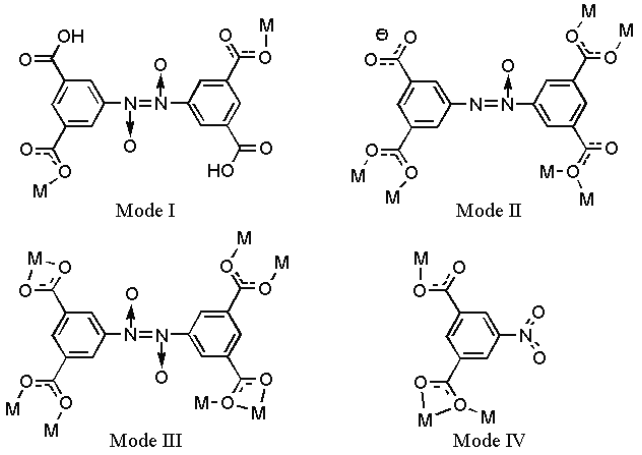

Scheme 2. The coordination modes of three H_4abtc oxidized derivatives in complex **1**–**4**.

The 1D $[Cd(nip)]_n$ ladder chains and the double helix $[Cd(bibp)]_n^{2n+}$ chains joined together by sharing the Cd^{II} ions, finally constructed a 3D framework (Fig. 4c). From a topology view, the framework of **4** can be rationalized to a 6−connected **6T8** net with the Point Schläfli symbol of $(4^4{\cdot}6^{11})$, in which $\{Cd_2(COO)_4\}$ binuclear SBUsact as 6−connected nodes, and all organic ligands as linkers (Fig. 4d).

Structural Comparison and Discussion. In the formation of the titled complexes, the H_4abtc displayed three oxidized derivatives, H_4Oabtc (one N atom was oxidized), H_4O_2abtc (two N atoms were oxidized), H_2nip (5-nitroisophthalic acid, one N atom were dioxidized), and the coordination modes are given in Scheme 2. The possible oxidation process of H_4abtc ligand under solvothermal conditions are given in the Scheme 1. The oxidation process is out of control, because the metal ions, organic solvents, as well as the bis(imidazole) ancially ligands can make the reaction activated. Not coincidentally, there are also some oxidazed H_4abtc ligands based coordination polymers have been reported. Hong and coworkers have been used the H_4o_2abtc ligands as pillars, constructed three Zn^{II} coordination polymers by adjust the reaction solvent and temperature, with the structure ranged from nonporous 2D→3D parallel entangled polycatenation to 3D microporous metal–organic framework.[10a] Li group also reported three H_4abtc ligand based Zn^{II} coordination polymers, in which the H_4abtc ligands also were oxidazed, with the final structures ranged from 1D chain to 3D framwork.[10b] Overall, we think the metal ions or SBUs, the solvent as well as the adjustion of bis(imidazole) ancially ligands cooperated with each other, make the H_4abtc oxidized derivatives based CPs possible.

In complex **1**, the H_4abtc exists in the H_4O_2abtc form, coordinated with two Co^{II} ions by using the $(\kappa^1\text{-}\kappa^0)\text{-}(\kappa^1\text{-}\kappa^0)\text{-}\mu_2$ mode, finally given a 2D+2D→3D parallel entangled network with the help of bridging bibp linkers. The dihedral angle between two phenyl rings is 5.74(0)°, indicating the whole $H_2O_2abtc^{2-}$ ligand was almost no twist. For complex **2**, although the existing form of H_4abtc is same with that in complex **1**, two phenyl rings rotated through the C−N bonds, with the dihedral angle is 76.76(2)°, almost vertical with each other, showing the $(\kappa^1\text{-}\kappa^1)\text{-}(\kappa^0\text{-}\kappa^2)\text{-}(\kappa^1\text{-}\kappa^1)\text{-}\mu_6$ coordination mode (Mode II). The rotated $Oabtc^{4-}$ ligand connected trinuclear $\{Mn_3(COO)_6\}$ SBUs, finally given a 2D (3,6)-connected $(4^3)_2(4^6{\cdot}6^6{\cdot}8^3)$−**kgd** network. And the cationized H_2bmib^{2+} ligands act as guest molecules in the formation of complex **2**. In complex **3**, two N atoms were oxidized, the H_4abtc ligand exhiting in the H_4O_2abtc form, adapted the $(\kappa^1\text{-}\kappa^1)\text{-}(\kappa^1\text{-}\kappa^1)\text{-}(\kappa^1\text{-}\kappa^2)\text{-}(\kappa^1\text{-}\kappa^1)\text{-}\mu_7$ coordination mode (Mode III), with the dihedral angle between two phenyl rings is

81.48(2)°. The O_2abtc^{4-} ligands linked the trinuclear $\{Cd_3(COO)_8\}$ SBUs, giving a 3D (4,8)−connected $(4^6)_2(4^{12}\cdot6^{12}\cdot8^4)$−**flu** framework. The cationized H_2bmib^{2+} ligands in complex **3** also act as guest molecules, and the trinuclear SBUs are similar with that in complex **2**. Thus, the difference between complexes **2** and **3** can mainly attributed to the oxidaztion degree of H_4abtc ligand. For complex **4**, when one N atom of azo group were dioxidized, the azo group (–N=N–) would broken, and the H_4abtc ligand degraded to the 5-nitroisophthalic acid (H_2nip), which adapted the $(\kappa^1\text{-}\kappa^0)\text{-}(\kappa^1\text{-}\kappa^2)\text{-}\mu_3$ coordination mode (Mode IV) in the construction of complex **4**, finally obtained a $\{Cd_2(COO)_4\}$ binuclear SBUs based 3D 6−connected $(4^4\cdot6^{11})$−**6T8** framework with the help of bridging bibp linkers. It is noteworthy that the $N_{nitro}\cdots N_{nitro}$ distance of two neighbouring chains is 3.280(4) Å, and the dihedral angle of two indenpdent phenyl rings is 0.0(0)°, which indicating the seperated nip^{2-} also have weak interaction with each other.

Minor chages can make big influences, the oxidation of the organic ligands make them have different perference in coordinated with metal or metal cluster based SBUs, finally constrcted stable complexes. And the ancillary ligands also have great effect on the diversity of the final packing structures.

Thermal Analyses. The thermogravimetric (TG) analyses were performed in N_2 atmosphere on polycrystalline samples of complex **1**–**4** and the TG curves are shown in Fig. S2. For complex **1**, the whole structure began to collapse around 380 °C, and then decomposes gradually. For **2**, the TGA curve shows the weight loss of 8.21 % up to 120 °C, which corresponds to the loss of coordinated and lattice water molecules (8.44 %). Subsequently, the loss of cationized H_2bmib^{2+} guest molecules took place in the range of 120-260 °C, and then and the complex is pyrolyzed. Similar with that in complex **2**, there are also three stages of weight loss in the sample collapses of complex **3**. The first weight loss of 5.17 % below 110 °C is ascribed to the release of lattice water molecules (4.97 %). And then the loss of cationized H_2bmib^{2+} guest molecules took place at about 180 °C. Further weight loss observed above 370°C indicates the decomposition of coordination framework. In the case of complex **4**, the weight loss of 1.46 % from 50 to 130°C is attributed to the loss of lattice water molecules (calc. 1.78 %). The weight loss corresponding to the release of organic ligands starts at 320°C with a result of thermal decomposition.

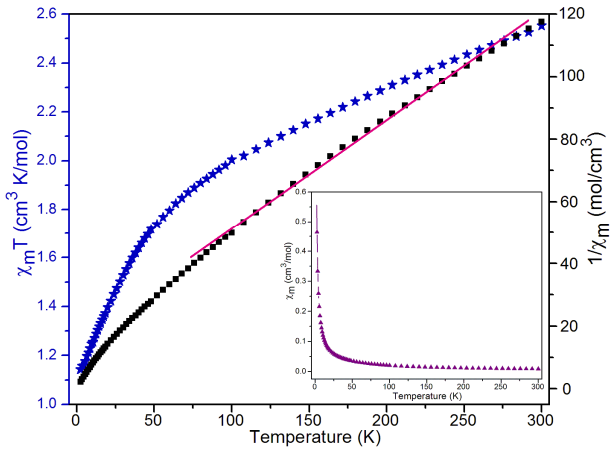

Figure 5. The temperature dependence of magnetic susceptibility of **1** under a static field of 1000 Oe.

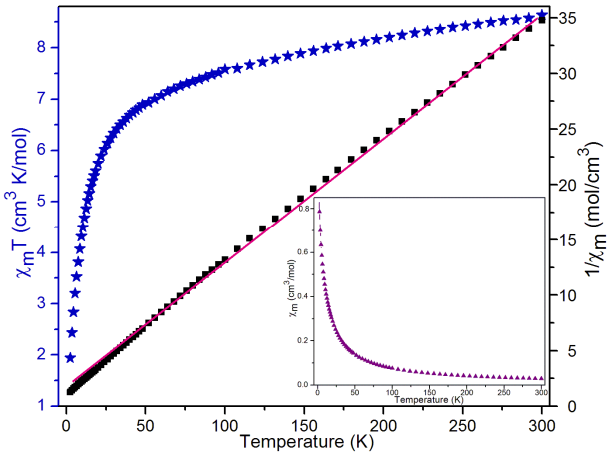

Figure 6. The temperature dependence of magnetic susceptibility of **2** under a static field of 1000 Oe.

Magnetic Property. The variable-temperature magnetic susceptibility measurements of complexes **1** and **2** in the form of $\chi_M T$, χ_M, $1/\chi_M$ vs T were performed in Fig. 5 and Fig. 6.

For complex **1**, the $\chi_M T$ value at room temperature is 2.55 cm^3 K mol^{-1}, is much larger than the 1.88 cm^3 K mol^{-1} value for a Co^{II} ion. This is probably induced by the presence of a strong orbital contribution in tetrahedral Co^{II}. With the temperature decreasing, the $\chi_M T$ value decreases continuously to 1.13 cm^3 K mol^{-1} at about 2K. The temperature dependence χ_M followed the Curie-Weiss law $\chi_M = C/(T-\theta)$ with C= 2.88 cm^3 K mol^{-1}, θ= –48.71 K (Fig. 5, inserted figure). And the negative value of θ also indicates the presence of an antiferromagnetic interaction exist between Co^{II} ions.

For complex **2**, the $\chi_M T$ value at room temperature is 8.64 cm^3 K mol^{-1}, lower than that for three spin-only magnetically isolated Mn^{II} ions (11.25 cm^3 K mol^{-1}), which can be attributed to the contribution to the susceptibility from orbital angular momentum at higher temperatures.[17] With the temperature decreasing, the $\chi_M T$ value decreases continuously to 1.69 cm^3 K mol^{-1} at about 2K. The temperature dependence χ_M followed the Curie-Weiss law $\chi_M = C/(T-\theta)$ with C= 8.70 cm^3 K mol^{-1}, θ= –10.79 K (Fig. 6, inserted figure), similar with the above reported ones. The negative value of θ also indicates the presence of an antiferromagnetic interaction exist between Mn^{II} ions.

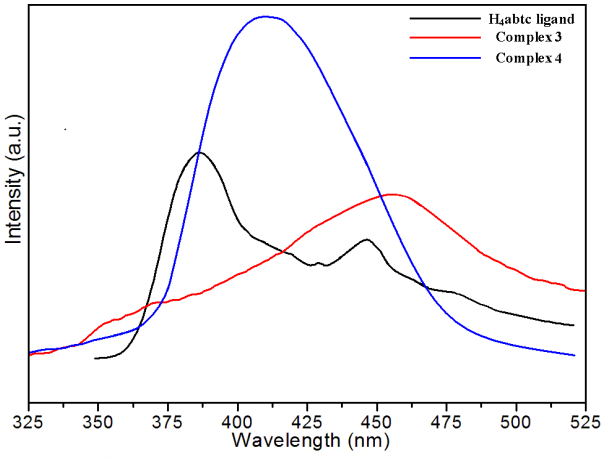

Figure 7. Solid-state emission spectra of H_4abtc ligand and complexes **3** and **4** at room temperature under 352 nm wavelength excitation.

Luminescent Properties. Many coordination compounds, especially the d^{10} metals based complexes, have been extensively studied due to their potential applications as luminescent materials.[18] The photoluminescent properties of H_4abtc and complexes **3** and **4** have been investigated under 352 nm wavelength excitation at room temperature, and the normalised photoluminescent spectres were shown in Fig.7.

For the ligand H_4abtc, two main emission bands at 385 nm and 446 nm, which can be attributed to the π*→n or π*→π transitions of aromatic rings. The emission spectra for **3** and **4** exhibit emission peaks of 458 and 410 nm, respectively, which may be assigned to the intraligand emission (π*→n or π*→π). These emissions are neither metal-to-ligand charge transfer (MLCT) nor ligand-to-metal transfer (LMCT) in nature since the Cd^{II} ion is difficult to oxidize or reduce due to its d^{10} configuration.[19] The differences of fluorescence properties between the H_4abtc ligand and two complexes probably derived from the different conformations of the oxidized H_4abtc ligands, which would make the conjugated system reduced. Besides, the different coordination environments of Cd^{II} ions also have the difference of the emission behaviours for complexes **3** and **4**, as the photoluminescence behaviour of CPs is closely associated with the metal ions and the ligands coordinated around them.[20]

Conclusions

In summary, four CPs were successfully designed and synthesized derived from the original ligand of 3,3',5,5'-azobenzenetetracarboxylic acid under solvothermal conditions, with a systematic variation of architectures from 2D (3,6)-connected **kgd** sheet (**2**), 2D+2D→3D 4-connected **sql** parallel entangled network (**1**), 3D (4,8)-connected **flu** net (**3**), to 3D 6-connected **6T8** framework (**4**). Detailed comparison of these networks reveals that the oxidation of the organic ligands as well as the ancillary ligands play important role on adjusting the structural diversity.

Acknowledgements. The work was supported by financial support from the Natural Science Foundation of China (Grant Nos. 21101097, 21451001), Natural Science Foundation of Shandong Province (ZR2010BQ023), key discipline and innovation team of Qilu Normal University.

Notes

The authors declare no competing financial interest.

References

1. (a) G. Férey and C. Serre, *Chem. Soc. Rev*., 2009, **38**, 1380; (b) M. Zhang, W. Lu, J. R. Li, M. Bosch, Y. P. Chen, T. F. Liu, Y. Liu and H. C. Zhou, *Inong. Chem. Front.*, 2014, **1**, 159; (c) B. L. Chen, N. W. Ockwig, A. R. Millward, D. S. Contreras and O. M. Yaghi, *Angew. Chem. Int. Ed*., 2005, **44**, 4745; (d) M. Kim, J. F. Cahill, H. Fei, K. A. Prather and S. M. Cohen, *J. Am. Chem. Soc*., 2012, **134**, 18082; (e) X. Zhang, L. Fan, Z. Sun, W. Zhang, W. Fan, L. Sun and X. Zhao, *CrystEngComm*, 2013, **15**, 4910; (f) S. L. Huang, A. Q. Jia and G. X. Jin, *Chem. Commun.*, 2013, **49**, 2403; (g) H. Li, Y. F. Han, Y. J. Lin, Z. W. Guo and G. X. Jin, *J. Am. Chem. Soc*., 2014, **136**, 2982; (h) D. S. Li, Y. P. Wu, J. Zhao, J. Zhang and J. Y. Lu, *Coord. Chem. Rev*., 2014, **261**, 1.
2. (a) E. D. Bloch, W. L. Queen, R. Krishna, J. M. Zadrozny, C. M. Brown and J. R. Long, *Science*, 2012, **335**, 1606; (b) S. Chen, R. Shang, K. L. Hu, Z. M. Wang and S. Gao, *Inong. Chem. Front.*, 2014, **1**, 83; (c) X. T. Zhang, D. Sun, B. Li, L. M. Fan, B. Li and P. H. Wei, *Cryst. Growth Des.*, 2012, **12**, 3845; (d) X. J. Kong, Y. Wu, L. S. Long, L. S. Zheng and Z. Zheng, *J. Am. Chem. Soc*., 2009, **131**, 6918; (e) W. Liu, X. Bao, L. L. Mao, J. Tucek, R. Zboril, J. L. Liu, F. S. Guo, Z. P. Ni and M. L. Tong, *Chem. Commun.*, 2014, **50**, 4059; (f) X. G. Guo, W. B. Yang, X. Y. Wu, Q. K. Zhang, L. Lin, R. Yu, H. F. Chen and C. Z. Lu, *Dalton Trans.,* 2013, **42**, 15106; (g) Z. M. Zhang, L. Y. Pan, W. Q. Lin, J. D. Leng, F. S. Guo, Y. C. Chen, L. J. Liu and M. L. Tong, *Chem. Commun*., 2013, **49**, 8081; (h) S. L. Huang, Y. J. Lin, T. S. A. Hor and G. X. Jin, *J. Am. Chem. Soc*., 2013, **135**, 8125.
3. (a) D. Sun, S. Yuan, H. Wang, H. F. Lu, S. Y. Feng and D. F. Sun, *Chem. Commun*., 2013, **49**, 6152; (b) X. T. Zhang, L. M. Fan, X. Zhao, D. Sun, D. C. Li and J. M. Dou, *CrystEngComm*, 2012, **14**, 2053; (c) J. J. Liu, Y. J. Lin and G. X. Jin, *Organometallics,* 2014, **33**, 1283; (d) J. B. Lin, W. Xue, B. Y. Wang, J. Tao, W. X. Zhang, J. P. Zhang and X. M. Chen, *Inorg. Chem*., 2012, **51**, 9423; (e) K. Wang, S. Zeng, H. Wang, J. Dou and J. Jiang, *Inong. Chem. Front.*, 2014, **1**, 167; (f) L. Fan, W. Fan, W. Song, G. Liu, X. Zhang and X. Zhao, *CrystEngComm*, 2014, **16**, 9191; (g) H. Yang, Q. X. Yao, Y. W. Li, D. C. Li and J. M. Dou, *Dalton Trans.,* 2014, **43**, 16986; (h) J. L. Liu, Y. C. Chen, Y. Z. Zheng, W. Q. Lin, L. Ungur, W. Wernsdorfer, L. F. Chibotaru and M. L. Tong, *Chem. Sci.*, 2013, **4**, 3310.
4. (a) D. Y. Du, J. S. Qin, S. L. Li, Z. M. Su and Y. Q. Lan, *Chem. Soc. Rev*., 2014, **43**, 4615; (b) S. Feng and R. Xu, *Acc. Chem. Res*., 2001, **34**, 239; (c) M. R. Gao, Y. F. Xu, J. Jiang and S. H. You, *Chem. Soc. Rev*., 2013, **42**, 2986.
5. (a) W. L. Leong and J. J.Vittal, *Chem. Rev.*, 2011, **111**, 688; (b) T. R. Cook, Y. R. Zheng and P. J. Stang, J. *Chem. Rev.*, 2013, **113**, 734; (c) X. Zhang, P. Wei, D. Sun, Z. Ni, J. Dou, B. Li, C. Shi and B. Hu, *Cryst. Growth Des.*, 2009, **9**, 4424; (d) W. Shi, S. Song and H. Zhang, *Chem. Soc. Rev*., 2013, **42**, 5714.
6. (a) A. N. Khlobystov, A. J. Blake, N. R. Champness, D. A. Lemenovskii, A. G. Majouga, N. V. Zyk and M. Schrpder, *Coord. Chem. Rev.*, 2001, **222**, 155; (b) N. Stock and S. Biswas, *Chem. Rev.*, 2012, **112**, 933.
7. (a) X. Zhang, L. Fan, W. Zhang, Y. Ding, W. Fan and X. Zhao, *Dalton Trans.,* 2013, **42**, 16562; (b) N. Zhang, Y. Tai, M. Liu, P. Ma, J. Zhao and J. Niu, *Dalton Trans.,* 2014, **43**, 5182; (c) U. J. Williams, B. D. Mahoney, A. J. Lewis, P. T. DeGregorio, P. J. Carroll and E. J. Schelter, *Inorg. Chem.*, 2013, **52**, 4142.
8. (a) J. J. Niu and D. Li, *Inorg. Chem. Commun.*, 2014, **339**, 119; (b) Y. B. Wang, Y. L. Lei, S. H. Chi and Y. J. Luo, *Dalton Trans.,* 2013, **42**, 1862; (c) X. Chang, J. Qin, M. Han, L. Ma and L. Wang, *CrystEngComm*, 2014, **16**, 870; (d) X. H. Chang, Y. Zhao, M. L. Han, L. F. Ma and L. Y. Wang, *CrystEngComm*, 2014, **16**, 6417; (e) L. P. Xue, C. X. Chang, S. H. Li, L. F. Ma and L. Y. Wang, *Dalton Trans.,* 2014, **43**, 7219; (f) M. L. Han, X. C. Chang, X. Feng, L. F. Ma and L. Y. Wang, *CrystEngComm*, 2014, **16**, 1687; (g) L. L. Liu, C. X. Yu, J. Sun, P. P. Meng, F. J. Ma, J. M. Du and L. F. Ma, *Dalton Trans.,* 2014, **43**, 2915.
9. (a) G. L. Liu and H. Liu, *CrystEngComm*, 2013, **15**, 6870; (b) C. Zhan, C. Zou, G. Q. Kong and C. D. Wu, *Cryst. Growth Des.*, 2013, **13**, 1429; (c) J. J. Wang, T. T. Wang, L. Tang, X. Y. Hou, L. J. Gao, F. Fu and M. L. Zhang, *J. Coord. Chem.*, 2013, **66**, 3979; (e) X. Chang, Y. Zhao, M. Han, L. Ma and L. Wang, *CrystEngComm*, 2014, **16**, 6417.
10. (a) M. Yan, F. Jiang, Q. Chen, Y. Zhou, R. Feng, K. Xiong and C. Hong, *CrystEngComm*, 2011, **13**, 3971; (b) J. Zhao, D. S. Li, X. J. Ke, B. Liu, K. Zou and H. M. Hu, *Dalton Trans.,* 2012, **41**, 2560; (c) W. Liu, L. Ye, X. Liu, L. Yuan, J. Jiang and C. Yan, *CrystEngComm*, 2008, **10**, 1395; (d) D. S. Li, X. J. Ke, J. Zhao, M. Du, K. Zou, Q. F. He and C. Li, *CrystEngComm*, 2011, **13**, 3355; (e) M. Meng, D. C. Zhong and T. B. Lu, *CrystEngComm*, 2011, **13**, 6794; (f) R. E. Osta, M. Frigoli, J. Marrot, N. Guillou, H. Chevreau, R. I. Walton and F. Millange, *Chem. Comm.*, 2012, **48**, 10639; (g) F. Xing, J. Jia, L. Liu, L. Zhong, M. Shao, Y. L. Bai, Y. Zhao, S. Zhu, X. He and M. Li, *CrystEngComm*, 2013, **15**, 4970; (h) X. S. Wang, S. Ma, K. Rauch, J. M. Simmons, D. Yuan, X. Wang, T. Yildirim,

W. C. Cole, J. J. Lopez, A. de Meijere and H. C. Zhou, *Chem. Mater.*, 2008, **20**, 3145.

11. (a) X. H. Chang, J. H. Qin, M. L. Han, L. F. Ma and L. Y. Wang, *CrystEngComm*, 2014, **16**, 8720; (b) L. Fan, X. Zhang, W. Zhang, Y. Ding, W. Fan, L. Sun, Y. Pang and X. Zhao, *Dalton Trans.,* 2014, **43**, 6701; (c) X. Zhang, L. Fan, W. Zhang, W. Fan, L. Sun and X. Zhao, *CrystEngComm*, 2014, **16**, 3203; (d) L. Fan, Y. Gao, G. Liu, W. Fan, W. Song, L. Sun, X. Zhao and X. Zhang, *CrystEngComm*, 2014, **16**, 7649; (e) T. Wu, Y. J. Lin and G. X. Jin, *Dalton Trans.*, 2014, **42**, 82; (f) W. Yang, C. Yang, Q. Ma, C. Li, H. Wang and J. Jiang, *CrystEngComm*, 2014, **16**, 4554; (g) L. Fan, W. Fan, W. Song, L. Sun, X. Zhao and X. Zhang, *Dalton Trans.,* 2014, **43**, 15979.
12. (a) T. Wu, Y. J. Lin and G. X. Jin, *Dalton Trans.*, 2014, **43**, 2356; (b) X. T. Zhang, L. M. Fan, Z. Sun, W. Zhang, D. C. Li, J. M. Dou and L. Han, *Cryst. Growth Des*., 2013, **13**, 792; (c) L. Fan, X. Zhang, Z. Sun, W. Zhang, Y. Ding, W. Fan, L. Sun, X. Zhao and H. Lei, *Cryst. Growth Des.*, 2013, **13**, 2462; (d) L. Fan, X. Zhang, W. Zhang, Y. Ding, L. Sun, W. Fan and X. Zhao, *CrystEngComm*, 2014, **16**, 2144; (e) Q. Ma, X. Feng, W. Cao, H. Wang and J. Jiang, *CrystEngComm*, 2013, **15**, 10383; (f) L. Zhang, J. Guo, Q. Meng, R. Wang and D. Sun, *CrystEngComm*, 2013, **15**, 9578.
13. (a) G. M. Sheldrick, *SHELXTL*, version 5.1; Bruker Analytical X-ray Instruments Inc.: Madison, WI, 1998. (b) G. M. Sheldrick, *SHELX-97*, PC Version; University of Gottingen: Gottingen, Germany, 1997.
14. (a) V. A. Blatov, A. P. Shevchenko and V. N. Serezhkin, *J. Appl. Crystallogr.*, 2000, **33**, 1193; (b) The network topology was evaluated by the program "TOPOS-4.0", see: http://www.topos.ssu.samara.ru. (c) V. A. Blatov, M. O'Keeffe and D. M. Proserpio, *CrystEngComm*, 2010, **12**, 44.
15. (a) P. Yang, M. S. Wang, J. J. Shen, M. X. Li, Z. X. Wang, M. Shao and X. He, *Dalton Trans.,* 2014, **43**, 1460; (b) Y. Q. Chen, S. J. Liu, Y. W. Li, G. R. Li, K. H. He, Z. Chang and X. H. B, *CrystEngComm*, 2013, **15**, 1613; (c) L. Liu, X. Lv, L. Zhang, L. Guo, J. Wu, H. Hou and Y. Fan, *CrystEngComm*, 2014, **16**, 8736.
16. (a) W. W. Dong, D. S. Li, J. Zhao, J. F. Ma, Y. P. Wu and Y. P. Duan, *CrystEngComm*, 2013, **15**, 5412; (b) L. Liu, X. Lv, L, Zhang, L. Guo, J. Wu, H. Hou and Y. Fan, *CrystEngComm*, 2014, **16**, 8736; (c) R. Luo, H. Xu, H. X. Gu, X. Wang, Y. Xu, X. Shen, W. Bao and D. R. Zhu, *CrystEngComm*, 2014, **16**, 784; (d) Y. P. Wu, D. S. Li, J. Zhao, Z. F. Fang, W. W. Dong, G. P. Yang and Y. Y. Wang, *CrystEngComm*, 2012, **14**, 4745; (e) S. Gao, R. Q. Fan, L. S. Qiang, P. Wang, S. Chen, X. M. Wang and Y. L. Yang, *CrystEngComm*, 2014, **16**, 1113.
17. (a) L. Fan, X. Zhang, D. Li, D. Sun, W. Zhang and J. Dou, *CrystEngComm*, 2013, **15**, 349; (b) L. L. Han, T. P. Hu, J. S. Chen, Z. H. Li, X. P. Wang, Y. Q. Zhao, X. Y. Li and D. Sun, *Dalton Trans.,* 2014, **43**, 8774; (c) Q. L. Zhang, P. Hu, Y. Zhao, G. W. Feng, Y. Q. Zhang, B. X. Zhu and Z. Tao, *J. Solid State Chem.*, 2014, **210**, 178; (d) L. L. Mao, W. Liu, Q. W. Li, J. H. Jia and M. L. Tong, *Cryst. Growth Des.*, 2014, **14**, 4674; (e) F. Liu, L. Zhang, R. Wang, J. Sun, J. Yang, Z. Chen, X. Wang, D. Sun, *CrystEngComm*, 2014, **16**, 2917; (f) L. Qin, M. Zhang, Q. Yang, Y. Li and H. Zheng, *Cryst. Growth Des*., 2013, **13**, 5045; (g) L. Qin, J. Hu, M. Zhang, Q. Yang, Y. Li and H. Zheng, *Cryst. Growth Des*., 2013, **13**, 2111.
18. (a) S. Yuan, Y. K. Deng, W. M. Xuan, X. P. Wang, S. N. Wang, J. M. Dou and D. Sun, *CrystEngComm*, 2014, **16**, 3829; (b) Y. Q. Zhao, M. X. Fang, Z. H. Xu, X. P. Wang, S. N. Wang, L. L. Han, X. Y. Li and D. Sun, *CrystEngComm*, 2014, **16**, 3015; (c) Z. H. Yan, L. L. Han, Y. Q. Zhao, X. Y. Liu, X. P. Wang, L. Wang and D. Sun, *CrystEngComm*, 2014, **16**, 8747; (d) J. J. Wang, T. T. Wang, L. Tang, X. Y. Hou, M. L. Zhang, L. J. Gao, F. Fu and Y. X. Ren, *Z. Anorg. Allg. Chem.*, 2014, **640**, 483; (e) C. Zhang, H. Hao, Z. Shi and H. Zheng, *CrystEngComm*, 2014, **16**, 5662.
19. (a) T. Liu, S. Wang, J. Lu, J. Dou, M. Niu, D. Li and J. Bai, *CrystEngComm*, 2013, **15**, 5476; (b) S. Wang, Y. Peng, X. Wei, Q. Zhang, D. Wang, J. Dou, D. Li and J. Bai, *CrystEngComm*, 2011, **13**, 5313; (c) Y. W. Li, S. J. Liu, T. L. Hu and X. H. Bu, *Dalton Trans.,* 2014, **43**, 11470; (d) F. Meng, L. Qin, M. Zhang and H. Zheng, *CrystEngComm*, 2014, **16**, 698; (e) Z. Ju, D. Cao, L. Qin, C. Zhang, M. Zhang, Z. Shi and H. Zheng, *CrystEngComm*, 2014, **16**, 3917; (f) L. Liu, J. Ding, M. Li, X. Lv, J. Wu, H. Hou and Y. Fan, *Dalton Trans.,* 2014, **43**, 12790; (g) L. P. Xue, X. H. Chang, S. H. Li, L. F. Ma and L. Y. Wang, *Dalton Trans.,* 2014, **43**, 7219; (h) L. L. Liu, C. X. Yu, J. Sun, P. P. Meng, F. J. Ma, J. M. Du and L. F. Ma, *Dalton Trans.,* 2014, **43**, 2915.
20. (a) S. Yuan, S. S. Liu and D. Sun, *CrystEngComm*, 2014, **16**, 1927; (b) X. Zhang, L. Fan, W. Song, W. Fan, L. Sun and X. Zhao, *RSC Adv.*, 2014, **4**, 30274; (c) G. Yu, N, Y, Li, X. Y. Ji, J. F. Wang, D. Liu and X. Y. Tang, *CrystEngComm*, 2014, **16**, 6621; (d) H. L. Jia, Z. Shi, Q. F. Yang, J. H. Yu and J. Q. Xu, *Dalton Trans.,* 2014, **43**, 5806; (e) H. R. Fu, F. Wang and J. Zhang, *Dalton Trans.,* 2014, **43**, 4668; (f) X. C. Yi, M. X. Huang, Y. Qi and E. Q. Gao, *Dalton Trans.,* 2014, **43**, 3691; (g) H. Jia, Y. Li, Z. Xiong, C. Wang and G. Li, *Dalton Trans.,* 2014, **43**, 3704; (h) J. Cui, Y. Li, Z. Guo and H. Zheng, *Chem. Commun.*, 2013, **49**, 555; (h) J. Yang, X. Wang, F. Dai, L. Zhang, R. Wang and D. Sun, *Inorg. Chem.,* 2014, **53**, 10649.

Dalton Trans.

For Table of Contents Use Only

Table of Contents Graphic and Synopsis

Structural Diversities and Related Properties of Four Coordination Polymers Synthesized From Original Ligand of 3,3',5,5'-Azobenzenetetracarboxylic Acid

Liming Fan, Weiliu Fan, Bin Li, Xinzheng Liu, Xian Zhao and Xiutang Zhang

Four CPs, derived from the original 3,3',5,5'-azobenzenetetracarboxylic acid ligand, have been obtained under solvothermal conditions.